

# Percolation and roughness in ballistic deposition of complex shapes

Linder C. DaSilva<sup>a</sup> and Marconi S. Barbosa<sup>a,\*</sup>

and Osvaldo N. Oliveira Jr.<sup>b</sup> and Luciano da F. Costa<sup>a</sup>

<sup>a</sup>*Cybernetic Vision Research Group Instituto de Física de São Carlos University of  
São Paulo 13560-970 São Carlos, SP, Brazil*

<sup>b</sup>*Polymer Research Group, DFCM-IFSC, Universidade de São Paulo, São Carlos,  
SP, Caixa Postal 369, 13560-970, Brasil*

---

## Abstract

This paper investigates how the measurement of geometrical features of structures obtained from ballistic deposition of objects with complex shapes, particularly neuronal cells, can be used for characterization and analysis of the shapes involved. The experiments were performed on both synthetic (prototypes) and natural shapes. Two measurements were considered, namely the surface roughness and the critical percolation density, with the former providing better discrimination of shape characteristics for alpha and beta neuronal cells of cat retina.

*Key words:* Morphometry, Neural Networks, Ballistic Deposition.

*PACS:* 87.80.Pa, 87.19.La

---

\* FAX: 55 16 273 9879, *email:* marconi@if.sc.usp.br

## 1 Introduction

Statistical mechanics has been extremely successful in connecting the emerging properties of a system of many elements to the microscopic description of its basic components. Because several natural systems involve basic elements with very simple geometry (point particles, for instance), relatively little attention has been given to systems containing elements with more complex geometry. Yet, understanding the statistics of complex shape elements is essential for a number of phenomena, especially in biology. A prototypical such situation is the central nervous system of animals, where a large number of neuronal cells, each with its intricate and particular shape, interconnect one another to produce emergent behavior. Indeed, neuronal cells are among the natural objects with the most complex shapes, which are required to make selective connections with close and distant targets [1]. The functional properties of a mature neuronal system are mainly determined by its synaptic weights, but the connecting pattern is ultimately a consequence of spatial interactions during the development of the system. Therefore, it is important to devise means to characterize the variety of neuronal shapes found in living beings. In addition, such morphological characterization can be used for classification in taxonomical studies (e.g. [2,3,4,5]) and for diagnosis of pathologies depending on neuronal shape alterations (e.g. [6,7]).

Several measurements have been proposed to characterize the morphology of complex shapes (e.g. [8,6,9,10]), but the analysis of complex aggregates found in Nature should also take into account the potential for interaction and contact between the constituent elements. Although several indirect measurements of the potential for contact between objects — including the ratio

between the squared perimeter and area of the basic elements, the fractal dimension [9,10,2] and lacunarity [11,12,13] — have been tried in the literature, only recently a more direct approach to the quantification of the connectivity potential between objects has been suggested [14,3]. A comparative discussion between percolation-based approaches and other more indirect measurements of cell morphology can be found in [14]. In the latter work, percolation was reached by establishing a connecting path between the left and right sides of a working space square, with the progressive addition of shapes to the square. In the case of neuronal cells, a connection was established during the simulation whenever a point of the dendrite was found to overlap a point of an axon. It has been suggested [14] that the critical density of elements characterizing percolation provides one of the most direct indications of the potential of those elements to form connected components. In case a single type of shape is used in the percolation simulations, it is possible to employ statistical mechanics to associate the intrinsic geometrical properties of the shape under analysis with the size of the emerging aggregates.

The present article investigates how the geometrical features of elements obtained with ballistic deposition [15,16,17] can be used to predict their potential for contact with each other. To our knowledge, this is the first use of ballistic deposition of elements assumed to have complex shapes for analysis of geometrical properties. Ballistic deposition is justified as an alternative model for characterizing neuronal (or any other shape) connectivity because it contemplates the biological situation where the growing neurites of migrating neuroblasts connect at the first contact with another neuronal cell. This feature is complementary to the approach reported in [14], in which the neurons are stamped one over the other, and to the more recent investigation of [18],

where the neurons are allowed to grow and percolate. Two measurements are considered to evaluate connectivity: the roughness of the aggregates surfaces and the critical percolation density.

The article starts by presenting the methodology adopted to simulate the ballistic deposition of aggregates and to obtain the corresponding measurements, after which the results are presented and discussed.

## 2 Methodology

In the standard on-lattice ballistic deposition model [15], a point particle is dropped from a randomly chosen position above the surface, located at a distance larger than the maximum height of the interface (the top surface of the aggregate in Figure 1). The particle follows a straight vertical trajectory until it reaches the surface of the aggregate, whereupon it sticks. The standard model has been extended to support the deposition of simple convex objects such as disks and spheres [19,20,15]. Such studies aimed essentially at describing the scaling properties of growing surface and not at characterizing the objects being deposited. The model developed here is an extension of traditional ballistic approaches, by considering the deposition of generic planar objects, such as neuronal cells, and investigating how geometrical features extracted from the aggregates – namely the roughness of the aggregate surface and the critical percolation density - can be used to characterize the shapes.

The surface roughness is a measure of fluctuation in the height of the interface

which can be defined as follows:

$$r(w, t) = \sqrt{\frac{1}{L} \sum_{i=1}^L [h(i, t) - \bar{h}(t)]^2} \quad (1)$$

Where  $\bar{h}(t)$  is the mean height of the aggregate surface and  $h(i, t)$  is the height of the column  $i$  of the lattice at time  $t$ . Note that the roughness is a function of time. The height values were obtained by thresholding the lattice image after applying the Distance Transform algorithm [21,8].

Percolation is a concept from statistical mechanics which corresponds to a phase transition in the system, as in the case of a cluster of deposited objects extending throughout the lattice connecting two lateral borders. This phenomenon is characterized in our simulation by the number of deposited objects at the percolation time.

In this study we considered 5 artificial planar objects and 61 planar neuronal cells, where the latter were normalized with respect to their diameter to minimize the effects from the different sizes of the objects. The artificial objects include several shapes to illustrate the percolation approach, while the natural objects refer to real neuronal cells from the cat retina.

Four data structures were used during the simulations: a matrix (`lattice`) 6000x1000 to store the objects, a vector (`surface`) to store the current height of each `lattice` column, and two lists (`flood_points` and `shape_points`), respectively, to check for percolation and to store the points of the current object being deposited.

The algorithm includes five main modules repeated in a loop, which are performed over the image points stored in `shape_points`:

- (1) Each object initiates its trajectory after having its center of mass to coincide, see Figure 1, with the position  $(x_{cm}, y_{cm})$ , where  $y_{cm}$  is the maximum height of the `lattice` and  $x_{cm}$  is generated from high-quality pseudo-random-number generator giving a uniform distribution between 0 and  $x_{max}$ .
- (2) The object is rotated between 0 and  $2\pi$ , around its center of mass.
- (3) In order to make it possible for the deposition of the object to occur, the `surface` is checked to determine the contact point. This is followed by updating the vector `lattice`, which stores every deposited object.
- (4) The roughness is computed.
- (5) The `lattice` is checked for percolation by running a flooding algorithm which tries to find a connected path from the left side of the lattice to the right side. If a connected path is found, the percolation has occurred; the number of deposited objects is recorded and execution is finished. Otherwise, the entire loop is repeated.

Two hundred simulations were performed for each case in order to compute the average percolation. All results have been obtained using an Openmosix cluster consisting of 10 Pentium IV 2.8 GHz and code developed in C++; each simulation needed about 15 hours of processor time to complete.

### 3 Results and Discussion

The procedure adopted to simulate ballistic deposition and assess connectivity is initially applied to the artificial shapes presented in Figure 2. These forms were chosen to illustrate how the gradual occupation of the Euclidean plane takes place: i) a ball with diameter of  $n$  pixels; ii) a cross with diameter of

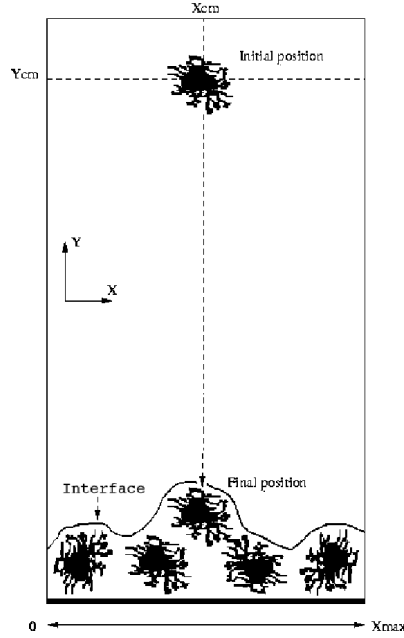


Fig. 1. Schematic representation of the systems used in simulations. Deposition is simulated on a rectangular grid with the surface at the bottom

$n$  pixels; iii) a line segment with  $n$  pixels; iv) a cross with area of  $n$  pixels (diameter  $n/2$ ); v) a ball with area of  $n$  pixels. An important issue is to identify the most important geometrical characteristic for percolation with ballistic deposition, whether it is the linear extension or the area. The analysis of percolation threshold should give an overall view of what to expect in cases with more general forms.

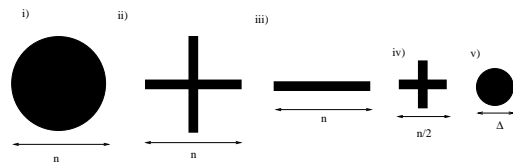


Fig. 2. Prototypical generic shapes used in the ballistic deposition computer experiment. The diameter  $\Delta$  in the last shape of this figure is defined by the constrained area of the circle which should match  $n$  pixels, i.e.  $\Delta = 2\sqrt{n/\pi}$

Figure 3 shows an example (realisation) of typical simulated chorals for each of the artificial shapes. Figure 4 shows the histogram of the critical number of

elements to achieve percolation for two hundred simulations for each shape.

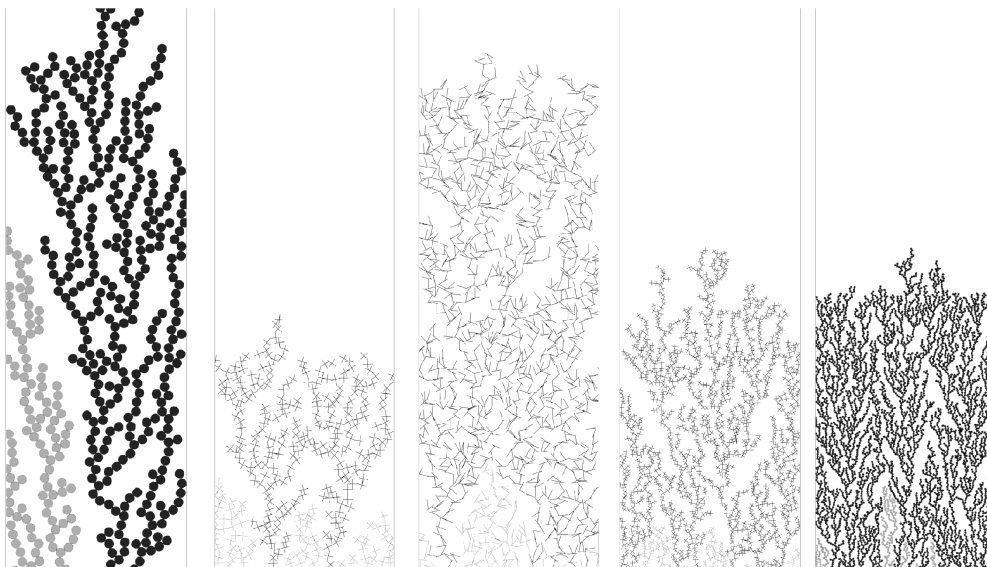


Fig. 3. A realization of the ballistic deposition percolation of the prototypical shapes considered in Figure 2. Connected groups in darker color correspond to the percolated cluster.

These histograms were fitted to a log-normal distribution curve, from which we extracted the global scalar features (e.g., the mean, the standard deviation, the maximum position, etc.). The first two of these measures were used to produce the scatter plot of Figure 5, which indicates that the morphology of the individual shapes plays an important role in determining the percolation threshold. As one could expect from the shapes investigated, the critical density varies considerably, with the large ball leading to percolation with the smallest number of objects (i.e. lowest density), while the highest critical density was obtained with the small ball. Note also that the average and the standard deviation of the critical densities are strongly correlated. As will be shown later, this correlation is maintained for more complex shapes.

Having observed a correlation between percolation threshold and shape for



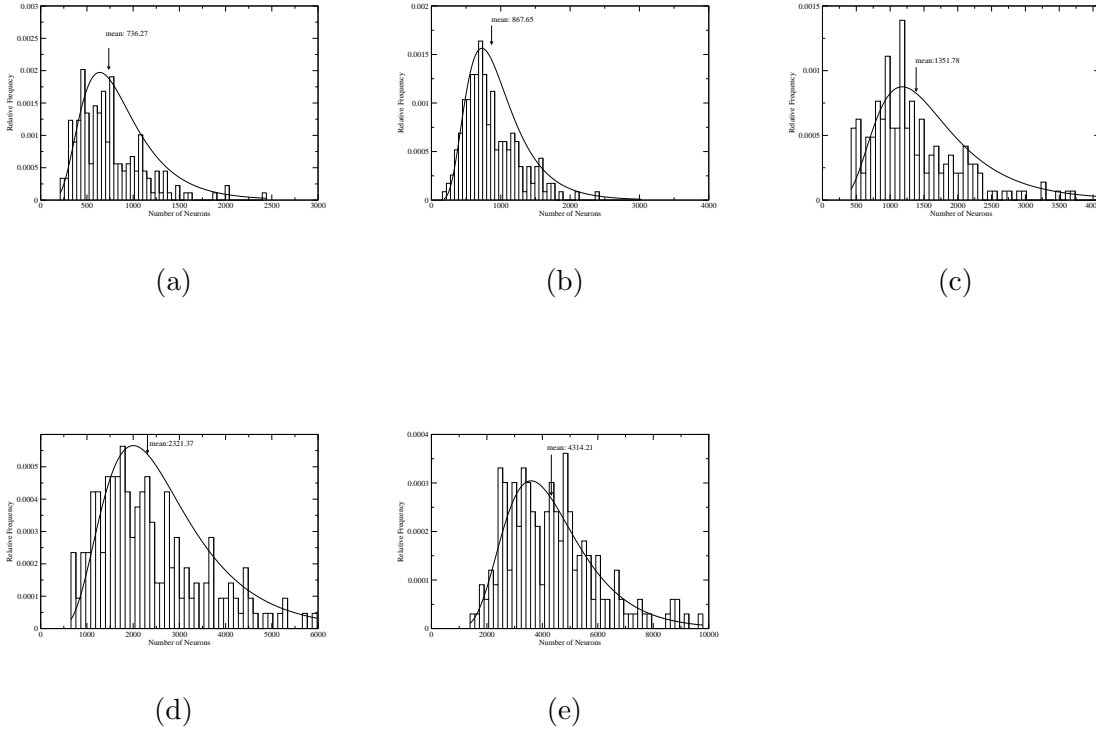


Fig. 4. Histograms from the computer simulation of the number of neurons required to achieve percolation for the prototypical chorals illustrated in Figure 3.

the artificial elements, we now proceed with the ballistic deposition of neuronal ganglion cells belonging to two of the main morphological/physiological classes of the domestic cat retina (alpha and beta classes). These are more complex shapes exhibiting limited, but definite, fractality [2]. Figure 6 illustrates a few examples of alpha and beta cells. There are a great variety of geometry characteristics among these cells even inside each class. In this paper we use the chorals grown by ballistic deposition as a toy model for the complex architecture of the actual cells in a mature network. The influence of cell shape at facilitating connectivity and on the surface properties is then directly associated with the potential for percolation.

Figure 7 shows two examples of chorals obtained by ballistic deposition of an

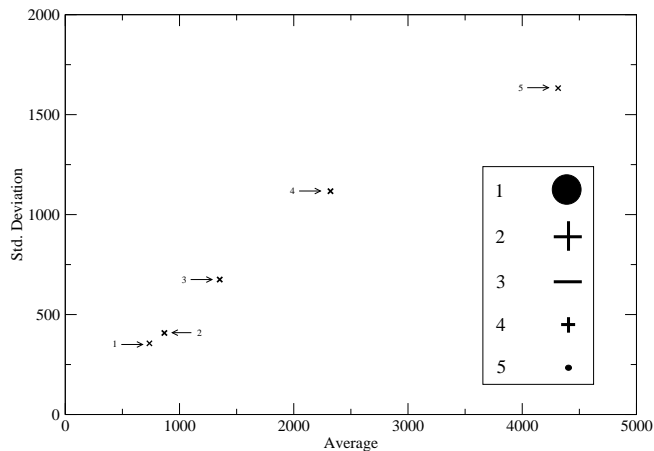


Fig. 5. A scatter plot based on the mean and standard deviation of the histograms of Figure 4, showing the influence of the geometry on percolation times.

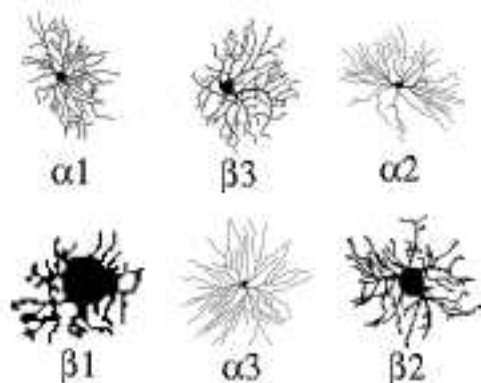


Fig. 6. Examples of the alpha and beta morphological classes of cat ganglion neuronal cells, three of each.

alpha and a beta cell displayed in Figure 6. As we did for the set of artificial cells, a sequence of two hundred simulations were performed for each of the cells in our database, with each simulation considering only a single cell. Histograms for the cells shown in Figure 6 are displayed in Figure 8. The average in each case, indicated by an arrow, tends to decrease from (a) to (f), indicating a clear decrease of the potential for connection of those cells.

With regard to the roughness of the aggregate surface, Figure 9 shows for

a few typical cells the almost linear increase in roughness with time up to 50 time units, which is chosen to correspond to the deposition of 10 objects (cells). In order to investigate the discriminative power of this measure, we produce a scatter plot shown in Figure 10, considering the slope of the curves of roughness vs. time for all cells in our database. O que esta figura mostra? O que estah na ordenada? Table 1 indicates that a Bayes classification analysis considering the roughness profile leads to a reasonable classification rate for the alpha cell type (88poorer discrimination of the beta cells (73involves estimating the density functions of each class of a training set of objects, weighted by the corresponding mass densities, and taking as the more likely class of a new object the class presenting the highest density for the specific set of measurements.

	$\alpha$	$\beta$	classification error
$\alpha$	21	3	0.12
$\beta$	10	26	0.27

Table 1

Bayes classification analysis considering the roughness profile displayed in Figure 10.

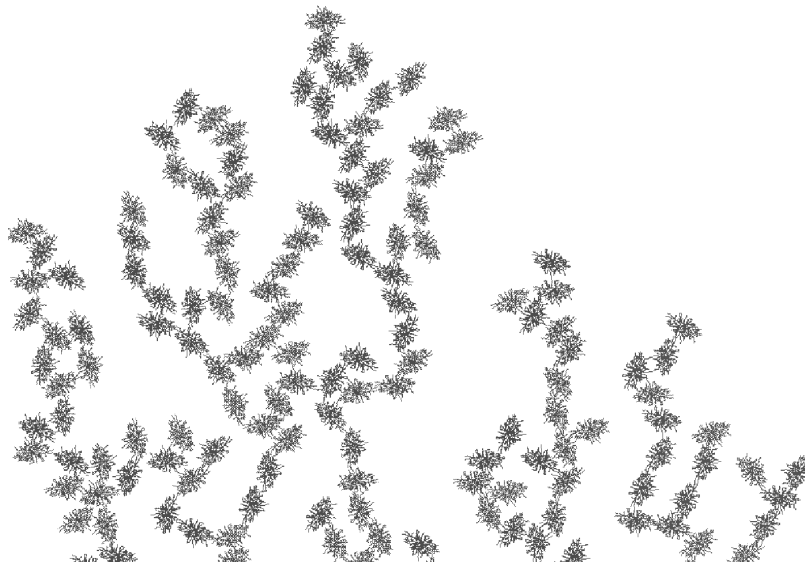
We now analyse whether the percolation index can also be used to discriminate between alpha and beta cells. This is carried out by extracting a series of global measurements such as the standard deviation and the mean from the histograms in order to produce a feature space or scatter plot. Figure 11 shows the scatter plots for all cells in our database of retinal cells (53 cells). It is clear from this scatter plot that while the retinal ganglion cells do share similarities, reflecting the known difficulty for visual classification, there is a clear division of the feature space populated by each kind of cells. This is

best illustrated by the density analysis shown in Figure 12. (o que estah nos eixos x e y da figura?) In addition, analogously to the results for the artificial shapes, such measurements are also highly correlated, suggesting that the correlation between the mean and the standard deviation could be a more general tendency. Table 2 shows the Bayesian classification considering the data in Figure 12, indicating classification rates slightly poorer than those obtained with the roughness measurements in Table 1.

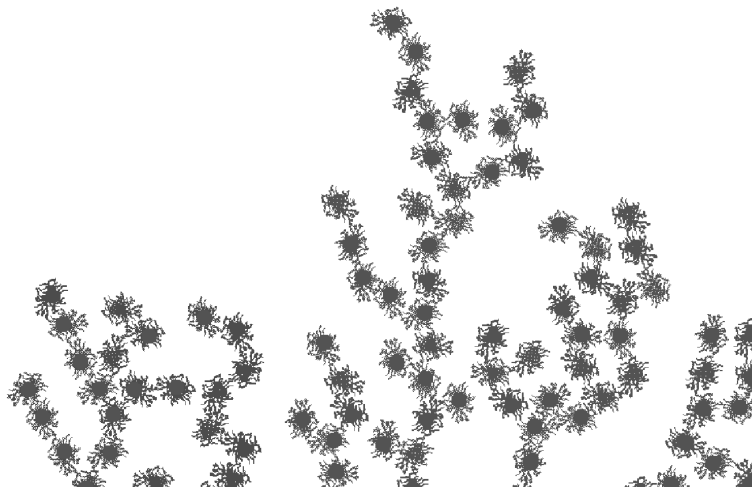
	$\alpha$	$\beta$	classification error
$\alpha$	20	4	0.16
$\beta$	15	21	0.41

Table 2

The result of a Bayes classification analysis considering the principal component profile displayed in Figure 12

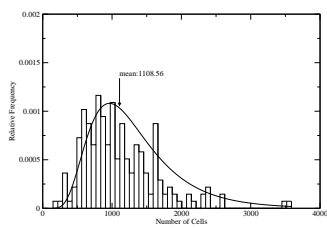


(a)

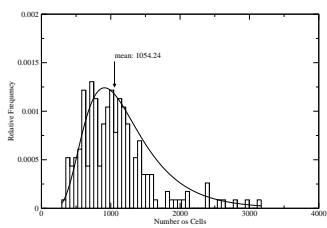


(b)

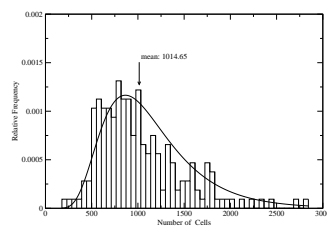
Fig. 7. Two examples of choral formation for representative examples of neuronal cells, one of each morphological class.



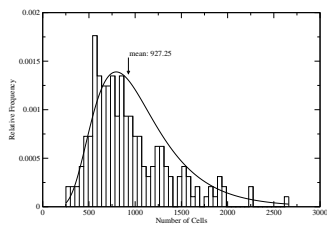
(a)



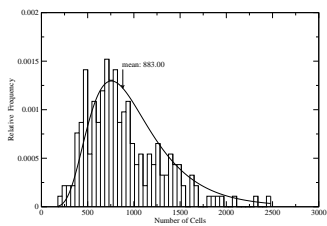
(b)



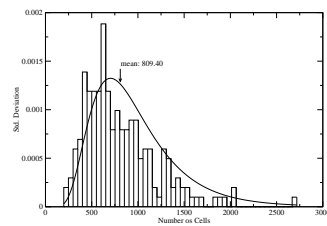
(c)



(d)



(e)



(f)

Fig. 8. Histograms from computer simulation for the six example cells shown in Figure 6, three of each morphological type.

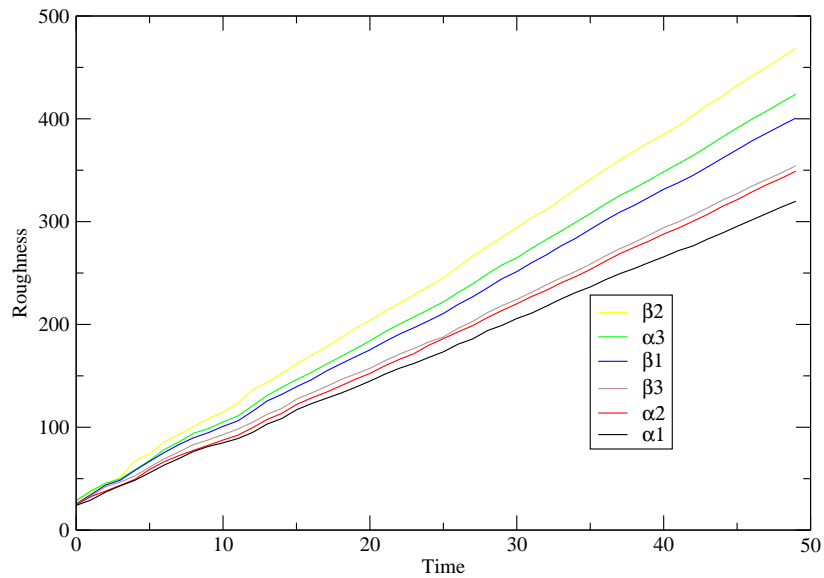


Fig. 9. The roughness of the aggregates for a few example cells as a function of the deposition time, showing the evolution of the sensitivity of this measure.

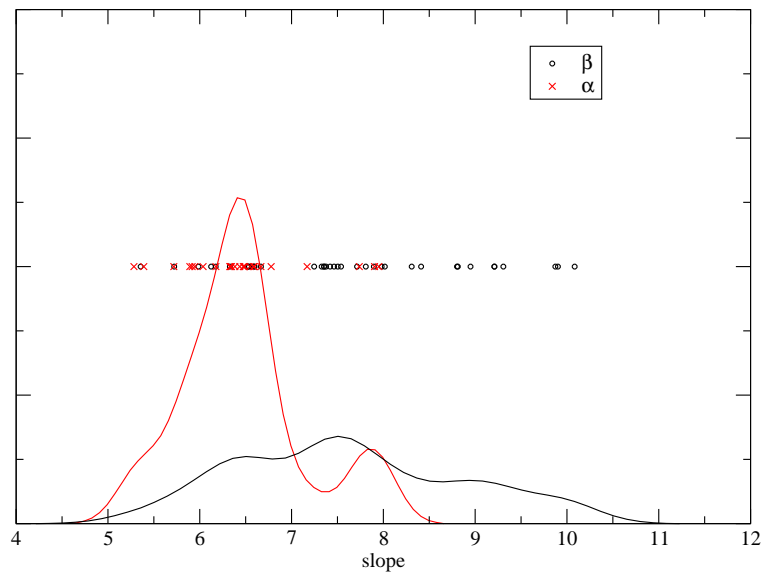


Fig. 10. A scatter plot based on the slope (in time) of roughness for the morphological classes alpha and beta. The density profile is also shown.

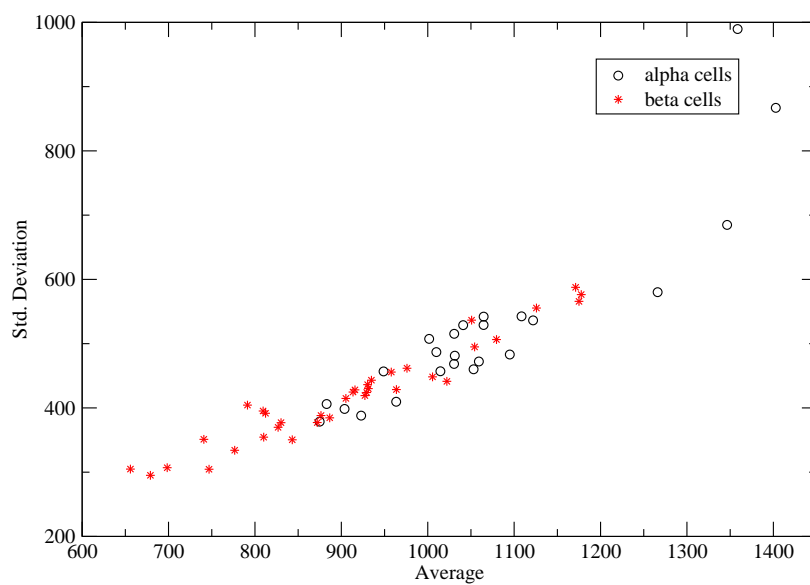


Fig. 11. A scatter plot defined by the mean and standard deviation values of the percolation index showing a reasonable separation of the morphological cell types alpha and beta.



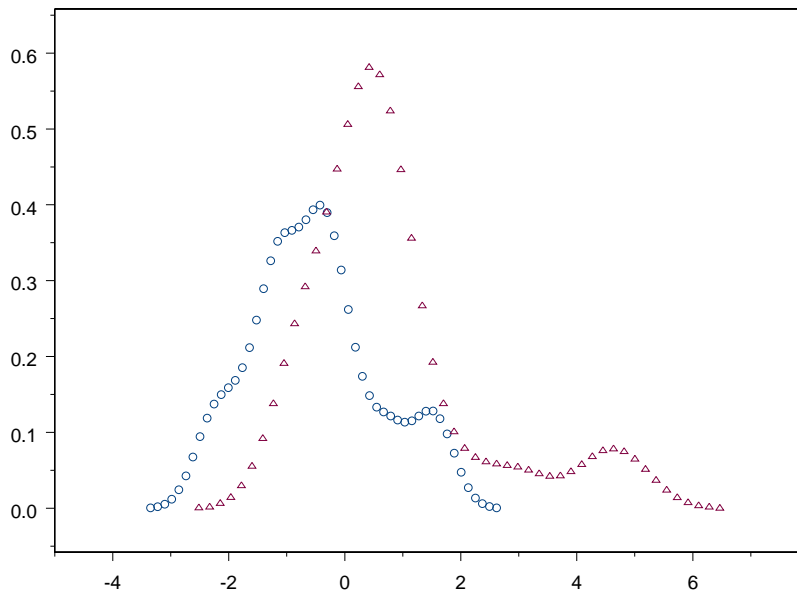


Fig. 12. Density profile for the first principal component of the measures defining the scatter plot in Figure 11, showing clearly distinguishable peaks for the two morphological classes. The curve with triangles represents the alpha cells and the other curve represents the beta cells.

## 4 Conclusions

The main aim of this work was to seek a means to quantify the potential for contact between objects with complex shapes. Pursuing further the suggestion to use the percolation critical density to quantify the potential of connection between neuronal shapes, as reported in [14], in the present work we addressed the critical density characterizing the percolation induced by the contacts between objects deposited in a ballistic process. While the percolation studies reported in [14] allowed overlap between parts of the objects <sup>1</sup>, the connections between objects in the present investigations are limited to take place by contact induced by the ballistic depositions. Therefore, such connections tend to occur between the most external parts of the objects. An immediate consequence is that the geometrical properties [4] of the interior of the cells become completely irrelevant to the critical densities used in this article. Thus, the percolation critical densities obtained in the current work provide a quantification of the potential of the objects to connect by contact, which is in principle different from the values obtained in [14] and [18].

In addition to the percolation critical densities, we also considered the use of the roughness of the aggregate surface as a possible measurement for characterizing neuronal morphology. The potential of both such features for discriminating between the two principal types of ganglion neuronal cells (namely  $\alpha$  and  $\beta$  morphological types) was also assessed in terms of Bayesian classification [8]. The discriminating ability upon using the percolation critical density

---

<sup>1</sup> In the case of neuronal cells, such overlaps would correspond to the fact that dendrites and/or axons in 3D spaces can deviate one another in order to establish connections with any part of the involved cells.

or the roughness of the aggregate surface can be objectively quantified in terms of the number of correct classifications. In this context, the two measurements led to similar performances, even though the roughness measurement had a slightly superior discrimination between the two types of cell, as shown in Figures 10 and 12 and Tables 1 and 2. Similarly to the results obtained in the previous approach reported in [18], the beta cells are more likely to engage in connections. Such an agreement between different percolation experiments, considering complementary types of connectivity, could be understood as an indication that the beta cells are optimized for enhanced connectivity.

Future investigations with the measurements considered in this article may involve applications to 3D objects and comparison with other measurements of shape morphology, such as shape functionals [4,7,22] and lacunarity [13].

## References

- [1] E. R. Kandel, J. H. Schwartz, and T. M. Jessell. *Principles of Neural Science*. Appleton & Lange, 1996.
- [2] L. F. Costa and T. J. Velte. Automatic characterization and classification of ganglion cells from the salamander retina. *Journal of Comparative Neurology*, 404:33–51, 1999.
- [3] L. F. Costa, M. S. Barbosa, and V. Coupez. A direct approach to neuronal connectivity. *Physica A*, 341:618–628, 2004.
- [4] M. S. Barbosa, L. F. Costa, and E. D. Bernardes. Neuromorphometric characterization with shape functionals. *Physical Review E*, 67(6), 2003.
- [5] C. L. Jones and H. F. Jelinek. Wavelet packet fractal analysis of neuronal

- morphology. *Methods*, 24(4):347–358, 2001.
- [6] L. F. Costa, E. T. Manoel, F. Faucereau, J. Chelly, J. van Pelt, and G. Ramakers. A shape analysis framework for neuromorphometry. *Journal of Comparative Neurology*, 13:282–310, 2002.
- [7] M. S. Barbosa, L. F. Costa, E. S. Bernardes, G. Ramakers, and J. van Pelt. Characterizing neuromorphologic alterations with additive shape functionals. *The European Physical Journal B*, 37:109–115, 2004.
- [8] L. F. Costa and R.M. Cesar-Jr. *Shape Analysis and Classification: Theory and Practice*. CRC Press, 2001.
- [9] PR. Montague and MJ Friedlander. Morphogenesis and territorial coverage by isolated mammalian retinal ganglion-cells. *Journal of Neuroscience*, 11(5):1440–1457, 1991.
- [10] L. F. Costa, A. G. Campos, and T. M. Manoel. An integrated approach to shape analysis: Results and perspectives. In *QCAV2001*, pages 23–34, 2001.
- [11] Mandelbrot B. B. *The Fractal Geometry of Nature*. W. H. Freeman, 1983.
- [12] Einstein A. J., Wu H. S., and Gil J. Self-affinity and lacunarity of chromatin texture in benign and malignant breast epithelial cell nuclei. *Phys. Rev. Lett.*, 80(2):397–400, 1998.
- [13] Rodrigues E. P., Barbosa M. S., and Costa L. da F. A self-referred approach do lacunarity. *submitted to Physical Review E*, 2004.
- [14] L. F. Costa and E. T. Manoel. A percolation approach to neural morphometry and connectivity. *Neuroinformatics*, 1(1):65–80, 2003.
- [15] A. L. Barabasi and H.E. Stanley. *Fractal Concepts in Surface Growth*. University of Cambridge, 1995.

- [16] D. N. Sutherland. Comment on vold's simulation of floc formation. *J. Colloid Interface Sci.*, 22:300–302, 1966.
- [17] M. J. Vold. Sediment volume and structure in dispersions of anisotropic particles. *J. Phys. Chem.*, 63:1608–1612, 1959.
- [18] Luciano da F. Costa and Regina C. Coelho. Growth-driven percolations: The dynamics of community formation in neuronal systems. *q-bio.NC/0411009*, 2004.
- [19] P. Meakin. Fractal aggregation. *Adv. Colloid Interface Sci.*, 28:249–331, 1988.
- [20] P. Viot, G. Tarjus, and J. Talbot. Exact solution of a generalized ballistic-deposition model. *Phys. Rev. E*, 48:480–488, 1993.
- [21] O. Cuisenaire and B. Macq. Fast euclidean distance transformation by propagation using multiple neighborhoods. *Computer Vision and Image Understanding*, 76:163–172, 1999.
- [22] L. da F. Costa, M. S. Barbosa, and V. Coupez. On the potential of the excluded volume and autocorrelation as neuromorphometric descriptors. *Physica A*, Available online, 2005.

